

Computational Analysis Over NACA-23015 Airfoil for Flow Separation Delay using Passive Flow Separation Techniques

S. Ram Sai*, K. Sai Priyanka**, R. Sabari Vihar***
UG student*, Assistant professor**, Assistant Professor***
Department of Aeronautical Engineering
Institute of Aeronautical Engineering, Hyderabad, India.

Abstract— Boundary layer is the layer of fluid in the immediate vicinity of a boundary surface where the effects of viscosity are significant. It is a thin layer of flowing gas or liquid in contact with a surface such that of an airplane wing or the inside of a pipe. Boundary layer separation is the detachment of a boundary layer from a surface into a wake. Separation occurs in flow that is slowing down, with pressure increasing, after passing through the thickest part of a streamline body, for example. A theoretical study on flow separation delay which involves methods using passive flow separation delay techniques is studied in this report. This report reviews the suction control over boundary layer method in depth there by making it easy to understand controlling of boundary layer separation. Analysis on Flow separation delay over NACA-23015 airfoil are conducted by varying velocity and Slots placement along the chord. This work helps further researchers in identifying and selecting the best position for suction Slots for better aerodynamic properties in designing a wing.

Keywords— Boundary layer, boundary layer separation, flow separation control.

I. INTRODUCTION

Boundary layer is the layer of fluid in the immediate vicinity of a boundary surface where the effects of viscosity are significant. It is a thin layer of flowing gas or liquid in contact with a surface such that of an airplane wing or the inside of a pipe. The aerodynamic boundary layer was first defined by Ludwig Prandtl in a paper presented on August 12, 1904 at the third International Congress of Mathematicians in Heidelberg, Germany. It simplifies the equations of fluid flow by dividing the flow field into two areas: one inside the boundary layer, dominated by viscosity and creating the majority of drag experienced by the boundary body. The pressure distribution throughout the boundary layer in the direction normal to the surface (such as an airfoil) remains constant throughout the boundary layer, and is the same as on the surface itself. The thickness of the velocity boundary layer is normally defined as the distance from the solid body to the point at which the viscous flow velocity is 99% of the free stream velocity (the surface velocity of an inviscid flow). Displacement thickness is an alternative definition stating that the boundary layer represents a deficit in mass flow compared to inviscid flow with slip at the wall. It is the distance by which the wall would have to be displaced in the inviscid case to give the same total mass flow as the viscous case.

Boundary layer separation is the detachment of a boundary layer from a surface into a wake. Separation occurs in flow that is slowing down, with pressure increasing, after passing through the thickest part of a streamline body, for example. The boundary layer separates when it has travelled far enough in an adverse pressure gradient that the speed of the boundary layer relative to the surface has stopped and reversed direction. The flow becomes detached from the surface, and instead takes the forms of eddies and vortices. The fluid exerts a constant pressure on the surface once it has separated instead of a continually increasing pressure if still attached. Flow separation results in reduced lift and increased pressure drag, caused by the pressure differential between the front and rear surfaces of the object.

Different studies have been undergone in order to delay the boundary layer separation of an airfoil at higher angle of attacks. Different methods and techniques were introduced to delay the boundary layer separation. The methods and techniques are as follows:

1. Streamlining the body shape
2. Suction control over boundary layer
3. Injecting high velocity fluid in boundary layer
4. Providing slots near leading edge of aircraft wing
5. Providing rotating cylinder at leading edge
6. Providing artificial roughness
7. Increasing velocity of fluid; etc.

A. Streamlining the body shape:

Providing a given body with a sleek shape that decreases the friction produced between the body and the fluid. Streamlined body shape helps the boundary layer to be attached longer than a rigid structure.

B. Suction control over boundary layer:

By providing a vacuum chamber or section at the internal portion of a body in order to reattach the separated boundary layer.

C. Injecting high velocity fluid in boundary layer:

Injecting high velocity fluid at the region of separation in order to increase the velocity of the oncoming fluid there by reattaching the separated boundary layer.

D. Providing slots near leading edge of aircraft wing:

By providing a slot at the leading edge of the aircraft wing we create a slot through which the oncoming fluid passes and reenergizes the boundary layer thereby reducing the boundary layer separation.

E. Providing rotating cylinder at leading edge:

By providing a rotating cylinder at the leading edge the lift coefficient is increased there by keeping the boundary layer attached to the surface of the wing compared to the normal design.

F. Providing artificial roughness:

Providing artificial roughness to a smooth surface it creates a small pocket where the fluid gets trapped and acts as a low-pressure region which helps the fluid flowing above to get attached to the surface there by reattaching the boundary layer.

G. Increasing velocity of fluid:

By increasing the velocity of the fluid, it affects the Reynolds number which in fact affects the boundary layer separation there by reattaching the separated boundary layer.

A theoretical study on flow separation delay which involves methods using passive flow separation delay techniques is studied and a method is proposed where the airfoil design is modified by inserting Slots and computational analysis is conducted in order to check the feasibility of the design to increase the angle of attack of the airfoil by reattaching the boundary layer to the airfoil. A passive method of reattachment of boundary layer is studied and executed.

II. METHODOLOGY

Analysis on Flow separation delay over NACA-23015 airfoil are conducted by varying velocity and Slots placement along the chord. Analysis was conducted on both the designs of airfoils i.e., on normal airfoil design and the Slotted airfoil. Computational analysis was done using ANSYS 2021 R1 Software. Models were created using Catia v6 and Fusion 360 software.

Coordinates of the airfoils were downloaded from airfoil tools website. Airfoils were designed along with an enclosure with 100mm chord length. Angle of Attack used were $0^\circ, 5^\circ, 10^\circ, 15^\circ, 20^\circ$. The dimensions of the enclosure are as follows; Length-400mm, Breadth-250mm, Arc radius-135mm.

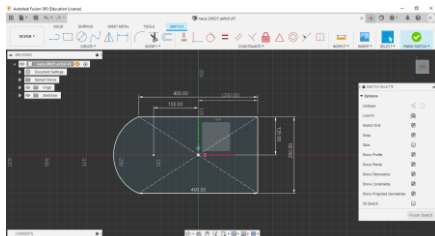


Figure1: Airfoil Designing Step-1

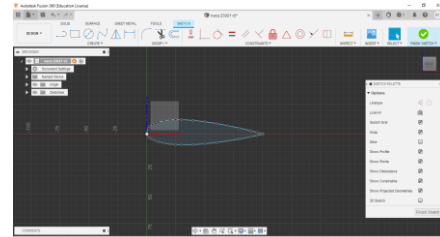


Figure2: Airfoil Designing Step-2

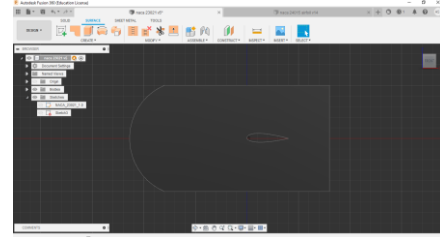


Figure3: Airfoil Designing Step-3

These models were imported to ANSYS and were computationally analyzed to get the values of coefficient of drag and coefficient of lift. The mesh to the imported geometry is given below.

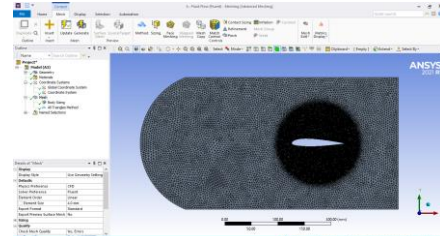


Figure4: Airfoil in Fluent Workbench Step-1

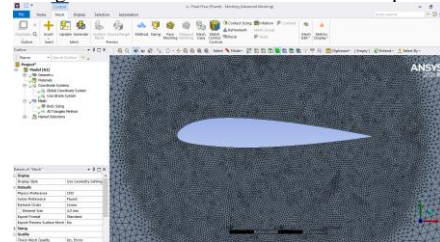


Figure5: Airfoil in Fluent Workbench Step-2

Calculations were done in ANSYS Fluent through which the Drag-Force, Lift-Force, Coefficient of Drag, Coefficient of Lift, were calculated. For 5m/s velocity Laminar model was used, 10m/s Spalart-Allmaras was used, 15m/s to 50 m/s K-epsilon and K-omega were used. Results were obtained for both the normal airfoil design and the airfoil with Slots.

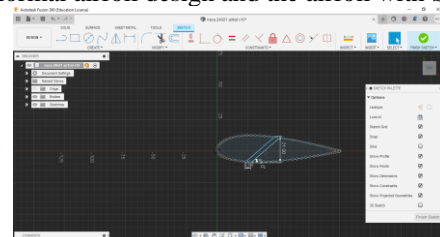


Figure6: Airfoil Designing with Slot Step-1

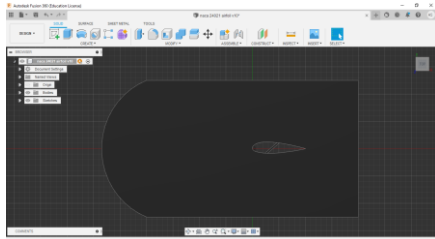


Figure7: Airfoil Designing with Slot Step-2

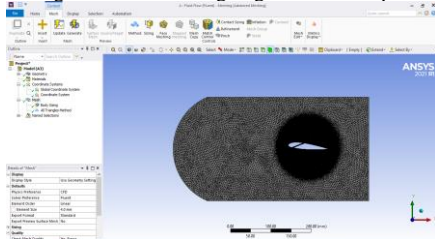


Figure8: Slotted Airfoil in Fluent Workbench Step-1

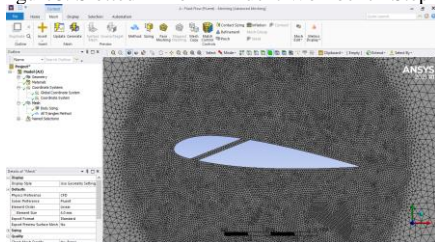


Figure9: Slotted Airfoil in Fluent Workbench Step-2

III. RESULTS

Calculations were done at 7 different velocities for 5 different angles of attack in order to compare the results obtained between the normal airfoils and the Slotted ones. The results for each airfoil at different AOA and velocities are as follows:

NACA 23015 Airfoil:

NACA 23015 Airfoil with Slot:

A. 0° Angle of Attack: -

1) 5m/s-

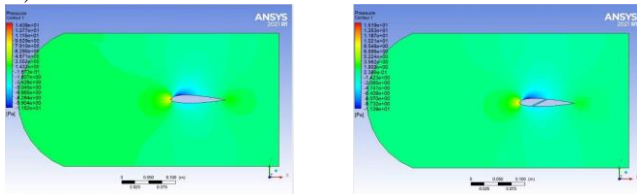


Figure10: Pressure Plot for Both with and Without Slot At 5m/s

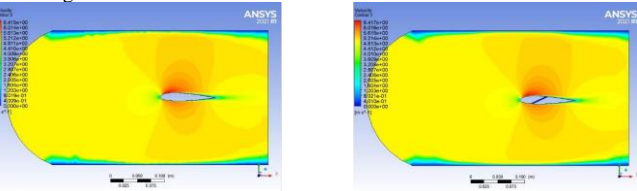


Figure11: Velocity Plot for Both with and Without Slot at 5m/s

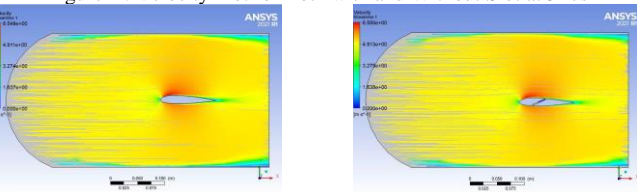


Figure12: Streamline for Both with and Without Slot at 5m/s

2) 25m/s-

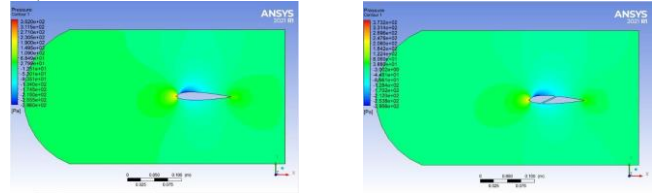


Figure13: Pressure Plot for Both with and Without Slot at 25m/s

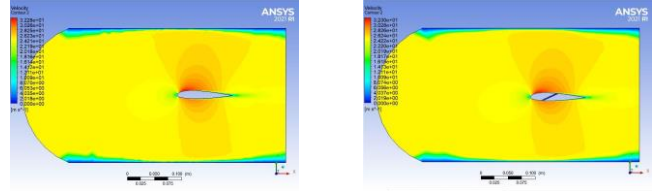


Figure14: Velocity Plot for Both with and Without Slot at 25m/s

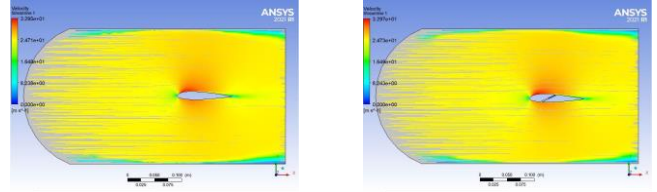


Figure15: Streamline for Both with and Without Slot at 25m/s

3) 50m/s-

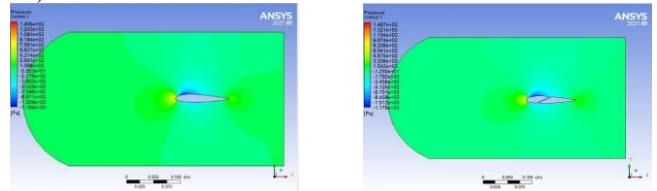


Figure16: Pressure Plot for Both with and Without Slot at 50m/s

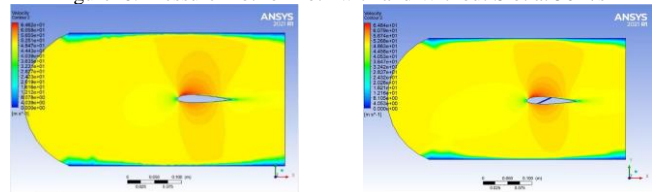


Figure17: Velocity Plot for Both with and Without Slot at 50m/s

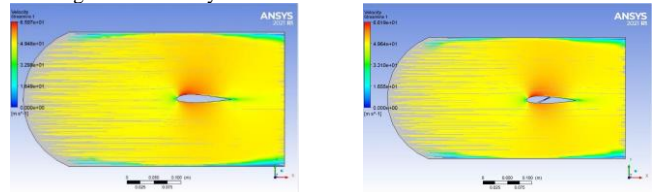


Figure18: Streamline for Both with and Without Slot at 50m/s

| Table of Design Points | | | | | | | | | |
|------------------------|----------------|-------------------|--------------|--------------------|--------------|--------------------|-------------------------------------|-------------------------------------|------|
| | A | B | C | D | E | F | G | H | I |
| 1 | Name | P1 - inlet | P2 - drag-up | P3 - drag-force-up | P4 - lift-up | P5 - lift-force-up | Retain | Retained Data | Note |
| 2 | Units | m s ⁻¹ | | N | | N | | | |
| 3 | DP 0 (Current) | 50 | 0.0018717 | 2.8661 | 0.011287 | 17.283 | <input checked="" type="checkbox"/> | <input checked="" type="checkbox"/> | |
| 4 | DP 1 | 30 | 0.00076614 | 1.4732 | 0.0039349 | 6.0254 | <input checked="" type="checkbox"/> | <input checked="" type="checkbox"/> | |
| 5 | DP 2 | 25 | 0.00055876 | 0.85559 | 0.0026974 | 4.1303 | <input checked="" type="checkbox"/> | <input checked="" type="checkbox"/> | |
| 6 | DP 3 | 20 | 0.00037975 | 0.56149 | 0.0016288 | 2.4941 | <input checked="" type="checkbox"/> | <input checked="" type="checkbox"/> | |
| 7 | DP 4 | 15 | 0.00023301 | 0.3568 | 0.00087203 | 1.3353 | <input checked="" type="checkbox"/> | <input checked="" type="checkbox"/> | |
| 8 | DP 5 | 10 | 0.00011869 | 0.18174 | 0.00036536 | 0.55945 | <input checked="" type="checkbox"/> | <input checked="" type="checkbox"/> | |
| 9 | DP 6 | 5 | 3.9189E-05 | 0.060009 | 8.1942E-05 | 0.12547 | <input checked="" type="checkbox"/> | <input checked="" type="checkbox"/> | |
| 10 | | | | | | | | | |

Figure19: Drag and Lift force values, Coefficient of Drag and lift values for NACA 23015 Airfoil at 0° AOA

| Table of Design Points | | | | | | | | | |
|------------------------|----------------|-------------------|------------|------------------|------------|------------------|-------------------------------------|-------------------------------------|------|
| | A | B | C | D | E | F | G | H | I |
| 1 | Name | P1-inlet | P2-drag-op | P3-drag-force-op | P4-lift-op | P5-lift-force-op | Retain | Retained Data | Note |
| 2 | Units | m s ⁻¹ | | N | | N | | | |
| 3 | DP 0 (Current) | 50 | 0.0021536 | 3.2976 | 0.0068552 | 10.497 | <input checked="" type="checkbox"/> | <input checked="" type="checkbox"/> | |
| 4 | DP 1 | 30 | 0.0008631 | 1.325 | 0.0023659 | 3.6227 | <input checked="" type="checkbox"/> | <input checked="" type="checkbox"/> | |
| 5 | DP 2 | 25 | 0.00062763 | 0.96091 | 0.0016085 | 2.4631 | <input checked="" type="checkbox"/> | <input checked="" type="checkbox"/> | |
| 6 | DP 3 | 20 | 0.00042454 | 0.63008 | 0.0010246 | 1.5889 | <input checked="" type="checkbox"/> | <input checked="" type="checkbox"/> | |
| 7 | DP 4 | 15 | 0.0002583 | 0.39552 | 0.00053867 | 0.80953 | <input checked="" type="checkbox"/> | <input checked="" type="checkbox"/> | |
| 8 | DP 5 | 10 | 0.00013015 | 0.19929 | 0.00018941 | 0.29003 | <input checked="" type="checkbox"/> | <input checked="" type="checkbox"/> | |
| 9 | DP 6 | 5 | 4.2902E-05 | 0.065693 | 5.8456E-05 | 0.08951 | <input checked="" type="checkbox"/> | <input checked="" type="checkbox"/> | |
| * | | | | | | | <input type="checkbox"/> | <input type="checkbox"/> | |

Figure20: Drag and Lift force values, Coefficient of Drag and lift values for NACA 23015 Airfoil with Slot at 0° AOA

B. 10° Angle of Attack: -

1)5m/s-

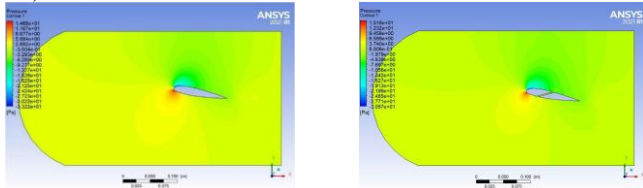


Figure21: Pressure Plot at 10° for Both with and Without Slot at 5m/s

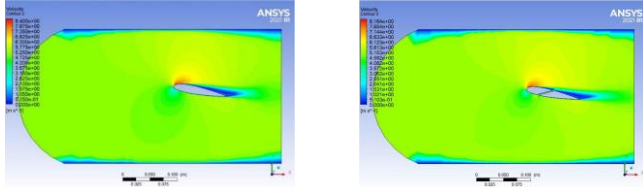


Figure22: Velocity Plot at 10° for Both with and Without Slot at 5m/s

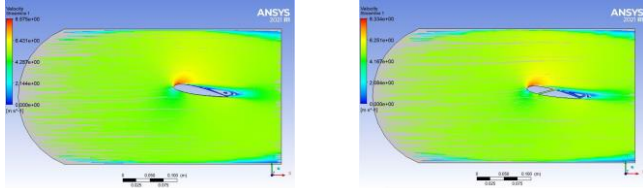


Figure23: Streamline at 10° for Both with and Without Slot at 5m/s

2)25m/s-

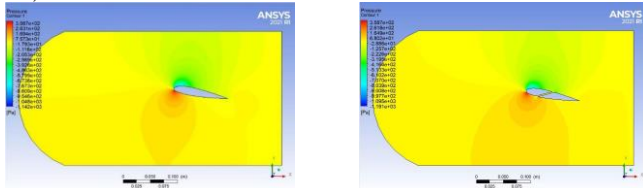


Figure24: Pressure Plot at 10° for Both with and Without Slot at 25m/s

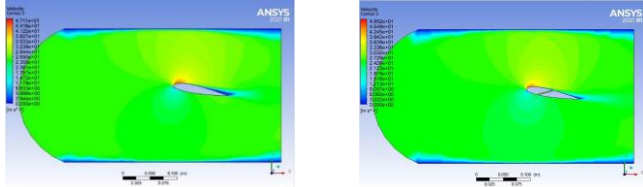


Figure25: Velocity Plot at 10° for Both with and Without Slot at 25m/s

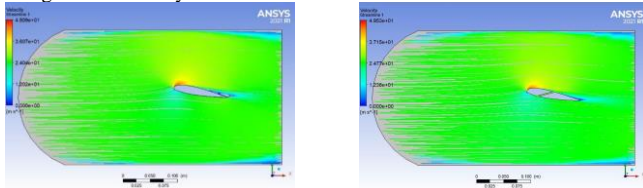


Figure26: Streamline at 10° for Both with and Without Slot at 25m/s

3)50m/s-

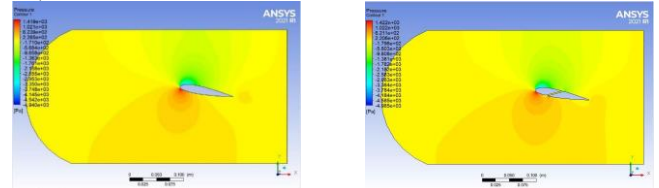


Figure27: Pressure Plot at 10° for Both with and Without Slot at 50m/s

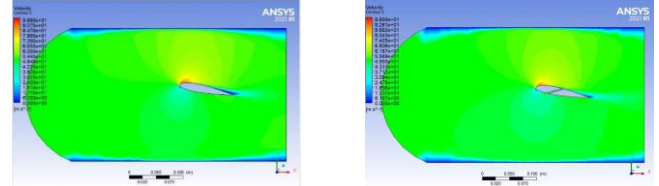


Figure28: Velocity Plot at 10° for Both with and Without Slot at 50m/s

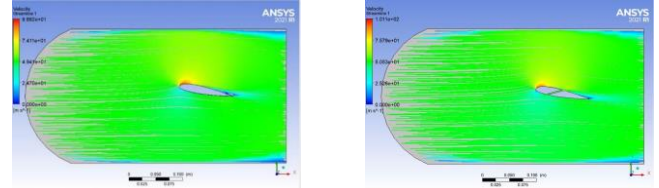


Figure29: Streamline at 10° for Both with and Without Slot at 50m/s

| Table of Design Points | | | | | | | | | |
|------------------------|----------------|-------------------|------------|------------------|------------|------------------|-------------------------------------|-------------------------------------|------|
| | A | B | C | D | E | F | G | H | I |
| 1 | Name | P1-inlet | P2-drag-op | P3-drag-force-op | P4-lift-op | P5-lift-force-op | Retain | Retained Data | Note |
| 2 | Units | m s ⁻¹ | | N | | N | | | |
| 3 | DP 0 (Current) | 50 | 0.0040105 | 6.141 | 0.10543 | 161.43 | <input checked="" type="checkbox"/> | <input checked="" type="checkbox"/> | |
| 4 | DP 1 | 30 | 0.0016087 | 2.4634 | 0.036364 | 55.682 | <input checked="" type="checkbox"/> | <input checked="" type="checkbox"/> | |
| 5 | DP 2 | 25 | 0.0011685 | 1.7892 | 0.024799 | 37.974 | <input checked="" type="checkbox"/> | <input checked="" type="checkbox"/> | |
| 6 | DP 3 | 20 | 0.00079545 | 1.218 | 0.015488 | 23.671 | <input checked="" type="checkbox"/> | <input checked="" type="checkbox"/> | |
| 7 | DP 4 | 15 | 0.00048803 | 0.74729 | 0.0083465 | 12.781 | <input checked="" type="checkbox"/> | <input checked="" type="checkbox"/> | |
| 8 | DP 5 | 10 | 0.00025179 | 0.38355 | 0.004532 | 5.2877 | <input checked="" type="checkbox"/> | <input checked="" type="checkbox"/> | |
| 9 | DP 6 | 5 | 8.1739E-05 | 0.12516 | 0.00075811 | 1.1609 | <input checked="" type="checkbox"/> | <input checked="" type="checkbox"/> | |
| * | | | | | | | <input type="checkbox"/> | <input type="checkbox"/> | |

Figure30: Drag and Lift force values, Coefficient of Drag and lift values for NACA 23015 Airfoil at 10° AOA

| Table of Design Points | | | | | | | | | |
|------------------------|----------------|-------------------|------------|------------------|------------|------------------|-------------------------------------|-------------------------------------|------|
| | A | B | C | D | E | F | G | H | I |
| 1 | Name | P1-inlet | P2-drag-op | P3-drag-force-op | P4-lift-op | P5-lift-force-op | Retain | Retained Data | Note |
| 2 | Units | m s ⁻¹ | | N | | N | | | |
| 3 | DP 6 (Current) | 50 | 0.0048885 | 7.4835 | 0.097052 | 148.61 | <input checked="" type="checkbox"/> | <input checked="" type="checkbox"/> | |
| 4 | DP 7 | 30 | 0.0018827 | 2.8892 | 0.033689 | 51.587 | <input checked="" type="checkbox"/> | <input checked="" type="checkbox"/> | |
| 5 | DP 8 | 25 | 0.0013525 | 2.071 | 0.023015 | 35.242 | <input checked="" type="checkbox"/> | <input checked="" type="checkbox"/> | |
| 6 | DP 9 | 20 | 0.00089746 | 1.3742 | 0.014405 | 22.058 | <input checked="" type="checkbox"/> | <input checked="" type="checkbox"/> | |
| 7 | DP 10 | 15 | 0.00053321 | 0.81647 | 0.0078413 | 12.007 | <input checked="" type="checkbox"/> | <input checked="" type="checkbox"/> | |
| 8 | DP 11 | 10 | 0.00026006 | 0.39822 | 0.0032905 | 5.0385 | <input checked="" type="checkbox"/> | <input checked="" type="checkbox"/> | |
| 9 | DP 12 | 5 | 8.0403E-05 | 0.12312 | 0.00072216 | 1.1058 | <input checked="" type="checkbox"/> | <input checked="" type="checkbox"/> | |
| * | | | | | | | <input type="checkbox"/> | <input type="checkbox"/> | |

Figure31: Drag and Lift force values, Coefficient of Drag and lift values for NACA 23015 Airfoil with Slot at 10° AOA

C. 20° Angle of Attack: -

1)5m/s-

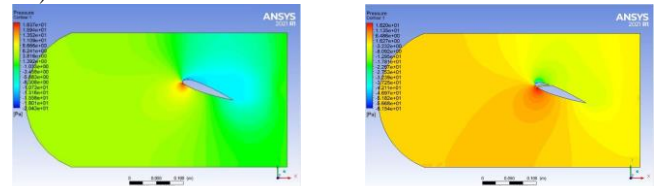


Figure32: Pressure Plot at 20° for Both with and Without Slot at 5m/s

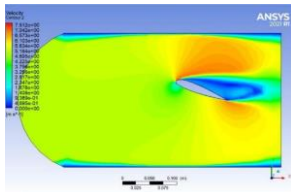


Figure33: Velocity Plot at 20° for Both with and Without Slot at 5m/s

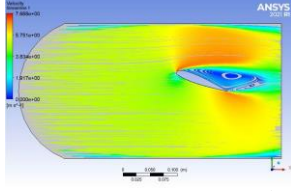


Figure34: Streamline at 20° for Both with and Without Slot at 5m/s

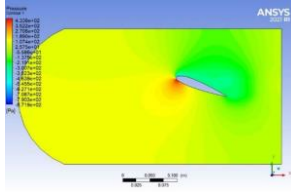


Figure35: Pressure Plot at 20° for Both with and Without Slot at 25m/s

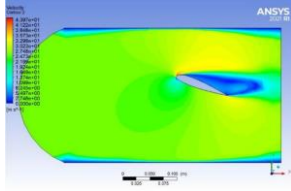


Figure36: Velocity Plot at 20° for Both with and Without Slot at 25m/s

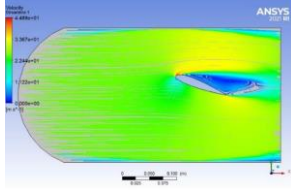


Figure37: Streamline at 20° for Both with and Without Slot at 25m/s

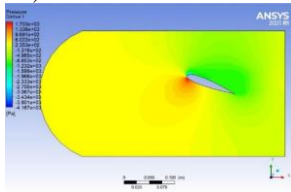


Figure38: Pressure Plot at 20° for Both with and Without Slot at 50m/s

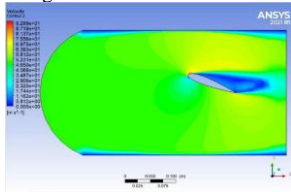


Figure39: Velocity Plot at 20° for Both with and Without Slot at 50m/s

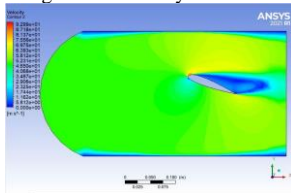


Figure40: Streamline at 20° for Both with and Without Slot at 50m/s

| Table of Design Points | | | | | | | | | |
|------------------------|----------------|-------------------|------------|------------------|------------|------------------|-------------------------------------|-------------------------------------|------|
| | A | B | C | D | E | F | G | H | I |
| 1 | Name | P1-inlet | P2-drag-up | P3-drag-force-up | P4-lift-up | P5-lift-force-up | Retain | Retained Data | Note |
| 2 | Units | m s ⁻¹ | | N | | N | | | |
| 3 | DP 0 (Current) | 50 | 0.01977 | 30.275 | 0.11954 | 183.04 | <input checked="" type="checkbox"/> | <input checked="" type="checkbox"/> | |
| 4 | DP 1 | 30 | 0.0074525 | 11.412 | 0.04195 | 64.236 | <input checked="" type="checkbox"/> | <input checked="" type="checkbox"/> | |
| 5 | DP 2 | 25 | 0.0033803 | 8.067 | 0.028949 | 44.175 | <input checked="" type="checkbox"/> | <input checked="" type="checkbox"/> | |
| 6 | DP 3 | 20 | 0.0034887 | 5.342 | 0.018043 | 27.628 | <input checked="" type="checkbox"/> | <input checked="" type="checkbox"/> | |
| 7 | DP 4 | 15 | 0.0020226 | 3.0972 | 0.009981 | 15.283 | <input checked="" type="checkbox"/> | <input checked="" type="checkbox"/> | |
| 8 | DP 5 | 10 | 0.00094556 | 1.4664 | 0.0042994 | 6.5834 | <input checked="" type="checkbox"/> | <input checked="" type="checkbox"/> | |
| 9 | DP 6 | 5 | 0.00026429 | 0.4047 | 0.00095596 | 1.5251 | <input checked="" type="checkbox"/> | <input checked="" type="checkbox"/> | |
| * | | | | | | | <input checked="" type="checkbox"/> | <input checked="" type="checkbox"/> | |

Figure41: Drag and Lift force values, Coefficient of Drag and lift values for NACA 23015 Airfoil at 20° AOA

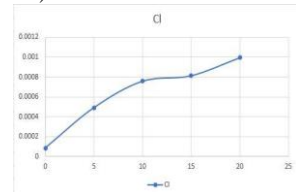
| Table of Design Points | | | | | | | | | |
|------------------------|----------------|-------------------|------------|------------------|------------|------------------|-------------------------------------|-------------------------------------|------|
| | A | B | C | D | E | F | G | H | I |
| 1 | Name | P1-inlet | P2-drag-up | P3-drag-force-up | P4-lift-up | P5-lift-force-up | Retain | Retained Data | Note |
| 2 | Units | m s ⁻¹ | | N | | N | | | |
| 3 | DP 0 (Current) | 50 | 0.016364 | 24.904 | 0.12847 | 196.72 | <input checked="" type="checkbox"/> | <input checked="" type="checkbox"/> | |
| 4 | DP 1 | 30 | 0.0060524 | 9.2693 | 0.045596 | 69.819 | <input checked="" type="checkbox"/> | <input checked="" type="checkbox"/> | |
| 5 | DP 2 | 25 | 0.0040627 | 6.5273 | 0.031455 | 48.166 | <input checked="" type="checkbox"/> | <input checked="" type="checkbox"/> | |
| 6 | DP 3 | 20 | 0.0027784 | 4.2544 | 0.019982 | 30.597 | <input checked="" type="checkbox"/> | <input checked="" type="checkbox"/> | |
| 7 | DP 4 | 15 | 0.0016057 | 2.4588 | 0.011126 | 17.037 | <input checked="" type="checkbox"/> | <input checked="" type="checkbox"/> | |
| 8 | DP 5 | 10 | 0.0007511 | 1.1501 | 0.0048215 | 7.3829 | <input checked="" type="checkbox"/> | <input checked="" type="checkbox"/> | |
| 9 | DP 6 | 5 | 0.00021349 | 0.3269 | 0.0011264 | 1.7248 | <input checked="" type="checkbox"/> | <input checked="" type="checkbox"/> | |
| * | | | | | | | <input checked="" type="checkbox"/> | <input checked="" type="checkbox"/> | |

Figure42: Drag and Lift force values, Coefficient of Drag and lift values for NACA 23015 Airfoil with Slot at 20° AOA

D. Graphs: -

NACA 23015 Airfoil

1) 5m/s-



NACA 23015 Airfoil with Slot

1) 5m/s-

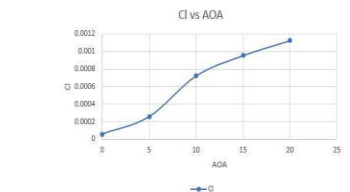


Figure43: Cl Vs AOA

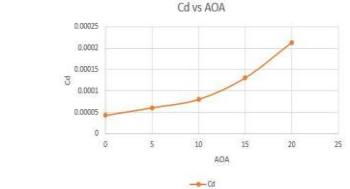
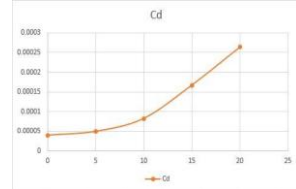


Figure44: Cd Vs AOA

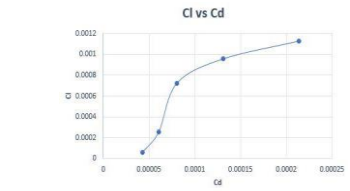
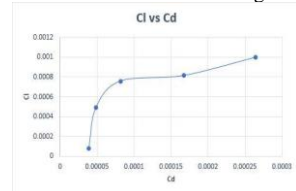


Figure45: Cl Vs Cd

2) 25m/s-

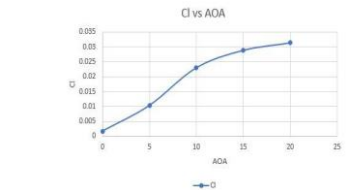
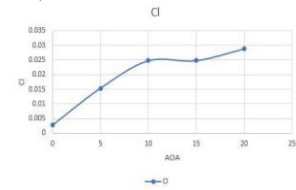


Figure46: Cl Vs AOA

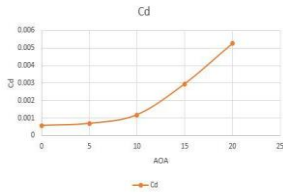


Figure47: Cd Vs AOA

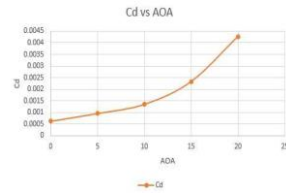


Figure48: Cl Vs Cd

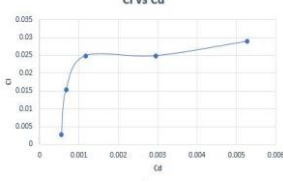


Figure49: Cl Vs AOA

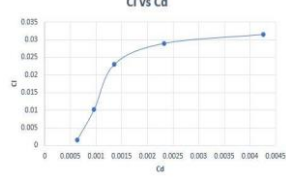


Figure50: Cd Vs AOA

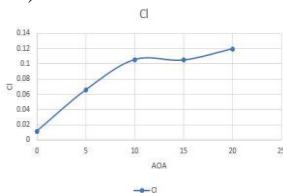
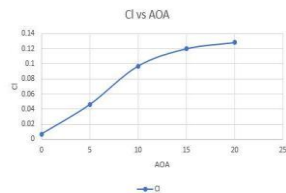


Figure51: Cl Vs Cd



3)50m/s-

From the above results of pressure plots, velocity plots, Streamline, Cl vs AOA, Cd vs AOA, Cl vs Cd graphs it is found that the airfoils with Slots show a greater lift force and coefficient of lift compared to the original designs. There is a slight reduction in the drag force and coefficient of drag produced in the Slotted airfoils than the original ones. From the observations we can infer that at higher Angles of Attack it is possible to attach the boundary layer to the upper surface of the airfoil by the Slots method there by increasing the lift produced and reducing the drag of an airfoil.

IV. DISCUSSION

The pressure contour and velocity contours are discussed with the principles that describes the velocity of air is passed through the domain in positive X direction, the air strike gets on the airfoil leading edge. After that, the air passed over the airfoil, due to tear off the air from influencing of airfoil shape. At the nose of the airfoil, the velocity is drastically reduced and pressure is increased.

At the nose of the airfoil pressure is 3 to 4 times higher than the atmospheric pressure. The upper surface flow velocity is high compared to lower surface flow, the upper surface creates a low pressure and low surface creates a high pressure.

Over the upper surface, the boundary layer has been formed due to viscosity and shear stress between air and airfoil surface. At the end of the trailing edge, the separation of the boundary layer is formed so that point pressure is reduced, velocity is increased.

It satisfied Bernoulli's principle, it states that an increase in the speed of a fluid occurs simultaneously with a decrease in static pressure or a decrease in the fluid's potential energy.

Lift force is continuously increased when the angle of attack is increased till the stall angle is achieved.

Drag force is proportional to angle of attack for all the cases analyzed. Separation of boundary layer on the upper surface is varying when the angle of attack is varied. Relative velocity is varying on upper and lower surface. Minimum drag coefficient occurs at a small positive angle of attack corresponding to a positive lift coefficient and builds only gradually at the lower angles.

It is observed during the process of methodology that there is an increase in the coefficient of lift and lift force and a decrease in drag force and coefficient of drag on the Slotted airfoils compared to the original airfoils. The passive flow separation method using Slots on the airfoils is helpful to reattach the separated boundary layer by which the airfoil can produce greater lift at an increased angle of attack of 20° without any help of high lift devices.

By placing the Slot inlet near to the 1/4th position the airfoil chord where there is a likely chance of formation of stagnation point at higher angles of attack the boundary layer is reattached to the airfoil by reenergizing the flow through the passage from the Slot. From the methodology the flow separation on the original airfoil design starts at 15° AOA whereas the flow is still attached on the Slotted airfoils.

At lower AOA the Slotted airfoils are not that useful as the flow gets distorted due to Slot there by decreasing the lift force and coefficient of lift and increasing the drag force and coefficient of drag. So Slotted airfoils are more useful at higher AOA's compared to lower AOAs by which we can deduce that the boundary layer is reattached successfully at higher AOAs to the Slotted airfoils compared to the original airfoils. Only the effective design and placements of the Slots are observed.

The AOA's and Velocities were restricted as this analysis mainly concerns the climb phase of aircrafts mission profile where the takeoff speed and AOA are not that high.

VI CONCLUSION

The flow simulation over the airfoil is successfully done for all cases. The drag force, lift force and their respective coefficients are successfully achieved. A contour plot for pressure and velocity is varying along the entire domain for all the different cases of observation.

A theoretical study on flow separation delay which involves methods using passive flow separation delay techniques is studied in this report. This report reviews the suction control over boundary layer method in depth thereby making it easy to understand controlling of boundary layer separation. Analysis on Flow separation delay over the airfoil are conducted by varying velocity and Slots placement along the chord.

Effective placement of Slots observed was at approximately nearer to 1/4th position of the chord length of the airfoil. Slotted airfoils are useful at higher angle of attack where the boundary

layer separates easily for the original airfoils. Only the effective design and placements of the Slots were shown in the results.

From the above results it is found that the airfoils with Slots show a greater lift force and coefficient of lift compared to the original designs. There is a slight reduction in the drag force and coefficient of drag produced in the Slotted airfoils than the original ones. From the observations we can infer that at higher Angles of Attack it is possible to attach the boundary layer to the upper surface of the airfoil by the Slots method thereby increasing the lift produced and reducing the drag of an airfoil.

ACKNOWLEDGMENT

I would like to take this opportunity to especially thank our guides, mentor and motivator Ms. K Sai Priyanka and Mr. R. Sabari Vihar for their interest towards me and for constant support included with trust that I can accomplish this task assigned to me. Respected mam and sir your actions have always been supportive and encouraging towards me which have been the most valuable assets in the completion of this work. I would like to once again thank you for your valuable contributions, insights, views and suggestion that have been of immense impact to me, I would forever cherish these moments.

REFERENCES

- [1]. H. ATIK , J. D. A. WALKER, "BOUNDARY-LAYER SEPARATION CONTROL USING LOCAL SUCTION" J. FLUID MECH. (2005), VOL. 535, PP. 415–443. C_2005 CAMBRIDGE UNIVERSITY PRESS DOI:10.1017/S002211200500501 X PRINTED IN THE UNITED KINGDOM
- [2]. HUA SHAN, ET. AL. "NUMERICAL STUDY OF PASSIVE AND ACTIVE FLOW SEPARATION CONTROL OVER A NACA0012 AIRFOIL" COMPUTERS & FLUIDS 37 (2008) 975–992
- [3]. A. Seifert, et.al, "Delay of Airfoil Stall by Periodic Excitation" JOURNAL OF AIRCRAFT Vol. 33, No. 4, July-August 1996
- [4]. Michael Amitay, et.al. "Aerodynamic Flow Control over an Unconventional Airfoil Using Synthetic Jet Actuators" AIAA JOURNAL Vol. 39, No. 3, March 2001
- [5]. J. C. Lin, F. G. Howard, and G.V.Selby, "Small Submerged Vortex Generators for Turbulent Flow Separation Control" VOL. 27, NO. 5, SEPT.-OCT. 1990. DOI: 10.2514/3.26172
- [6]. LaTunia Pack Melton, Chung-Sheng Yao, and Avi Seifert "Active Control of Separation from the Flap of a Supercritical Airfoil" AIAA JOURNAL Vol. 44, No. 1, January 2006 DOI: 10.2514/1.12225
- [7]. P R VISWANATH, "some thoughts on separation control strategies" Sadhan a Vol. 32, Parts 1 & 2, February–April 2007, pp. 83–92. © Printed in India
- [8]. Reynald Buret.al. "Separation control by vortex generator devices in a transonic channel flow" Shock Waves (2009) 19:521-530 DOI: 10.1007/s00193-009-0234-6
- [9]. Hirotoshi Fujieda, Hitoshi Takahashi et.al. "Aerodynamic Development of Boundary Layer Control System for NAL QSTOL Research Aircraft 'ASKA'" International Pacific Air & Space Technology Conference DOI: 10.4271/912010
- [10]. Mathieu Sellier and Wei Hua Ho, "Eliminating Boundary Layer Separation on a Cylinder with Non-uniform Suction" International Journal of Aerospace Engineering / 2020 / Article doi: 10.1155/2020/9137369
- [11]. Jose Rodriguez and Dominique Rothan "Low Reynolds Number Laminar Separation Bubble Control Using a Backward Facing Step" Aerospace Technology Conference and Exposition DOI: 10.4271/932572
- [12]. Hiroshi Yokoyama, et.al. "Experimental and Numerical Investigations on Control Methods of Cavity Tone by Blowing Jet in an Upstream Boundary Layer" Noise and Vibration Conference and Exhibition DOI:10.4271/2017-01-1786
- [13]. Ralph J. Volino, "SEPARATION CONTROL ON LOW-PRESSURE TURBINE AIRFOILS USING SYNTHETIC VORTEX GENERATOR JETS" Proceedings of ASME Turbo Expo 2003 Power for Land, Sea, and Air June 16-19, 2003, Atlanta, Georgia, USA. GT2003-38729
- [14]. J. C. Lin, et.al. "Turbulent Flow Separation Control Through Passive Techniques" AIAA 2nd Shear Flow Conference March 13-16, 1989 / Tempe, AZ